

Passivation and dissociation of P_b-type defects at a-SiO_2/Si interface

Xue-Hua Liu(刘雪华), Wei-Feng Xie(谢伟锋), Yang Liu(刘杨), and Xu Zuo(左旭)
Citation: Chin. Phys. B, 2021, 30 (**9**): 097101. DOI: 10.1088/1674-1056/ac0e20
Journal homepage: http://cpb.iphy.ac.cn; http://iopscience.iop.org/cpb

What follows is a list of articles you may be interested in

Magnetic and electronic properties of two-dimensional metal-organic frameworks $TM_3(C_2NH)_{12}$

Zhen Feng(冯振), Yi Li(李依), Yaqiang Ma(马亚强), Yipeng An(安义鹏), and Xianqi Dai(戴宪起)
Chin. Phys. B, 2021, 30 (**9**): 097102. DOI: 10.1088/1674-1056/ac0cdb

Bilayer twisting as a mean to isolate connected flat bands in a kagome lattice through Wigner crystallization

Jing Wu(吴静), Yue-E Xie(谢月娥), Ming-Xing Chen(陈明星), Jia-Ren Yuan(袁加仁), Xiao-Hong Yan(颜晓红), Sheng-Bai Zhang(张绳百), and Yuan-Ping Chen(陈元平)
Chin. Phys. B, 2021, 30 (**7**): 077104. DOI: 10.1088/1674-1056/abd7d6

Cobalt anchored CN sheet boosts the performance of electrochemical CO oxidation

Xu Liu(刘旭), Jun-Chao Huang(黄俊超), and Xiang-Mei Duan(段香梅)
Chin. Phys. B, 2021, 30 (**6**): 067104. DOI: 10.1088/1674-1056/abfbd7

Investigation of electronic, elastic, and optical properties of topological electride Ca_3Pb via first-principles calculations

Chang Sun(孙畅), Xin-Yu Cao(曹新宇), Xi-Hui Wang(王西惠), Xiao-Le Qiu(邱潇乐), Zheng-Hui Fang(方铮辉), Yu-Jie Yuan(袁宇杰), Kai Liu(刘凯), and Xiao Zhang(张晓)
Chin. Phys. B, 2021, 30 (**5**): 057104. DOI: 10.1088/1674-1056/abec38

First-principles calculations of K-shell x-ray absorption spectra for warm dense ammonia

Zi Li(李孜), Wei-Jie Li(李伟节), Cong Wang(王聪), Dafang Li(李大芳), Wei Kang(康炜), Xian-Tu He(贺贤土), and Ping Zhang(张平)
Chin. Phys. B, 2021, 30 (**5**): 057102. DOI: 10.1088/1674-1056/abdb1b

---

RAPID COMMUNICATION

Passivation and dissociation of P_b-type defects at a-SiO_2/Si interface*

Xue-Hua Liu(刘雪华)[1], Wei-Feng Xie(谢伟锋)[1], Yang Liu(刘杨)[2,3], and Xu Zuo(左旭)[1,4,5,†]

[1] College of Electronic Information and Optical Engineering, Nankai University, Tianjin 300350, China
[2] Microsystem and Terahertz Research Center, China Academy of Engineering Physics, Chengdu 610200, China
[3] Institute of Electronic Engineering, China Academy of Engineering Physics, Mianyang 621999, China
[4] Key Laboratory of Photoelectronic Thin Film Devices and Technology of Tianjin, Nankai University, Tianjin 300350, China
[5] Engineering Research Center of Thin Film Optoelectronics Technology, Ministry of Education, Nankai University, Tianjin 300350, China

(Received 2 June 2021; revised manuscript received 19 June 2021; accepted manuscript online 24 June 2021)

It is well known that in the process of thermal oxidation of silicon, there are P_b-type defects at amorphous silicon dioxide/silicon (a-SiO_2/Si) interface due to strain. These defects have a very important impact on the performance and reliability of semiconductor devices. In the process of passivation, hydrogen is usually used to inactivate P_b-type defects by the reaction $P_b + H_2 \rightarrow P_bH + H$. At the same time, P_bH centers dissociate according to the chemical reaction $P_bH \rightarrow P_b + H$. Therefore, it is of great significance to study the balance of the passivation and dissociation. In this work, the reaction mechanisms of passivation and dissociation of the P_b-type defects are investigated by first-principles calculations. The reaction rates of the passivation and dissociation are calculated by the climbing image-nudged elastic band (CI-NEB) method and harmonic transition state theory (HTST). By coupling the rate equations of the passivation and dissociation reactions, the equilibrium density ratio of the saturated interfacial dangling bonds and interfacial defects (P_b, P_{b0}, and P_{b1}) at different temperatures is calculated.

Keywords: first-principles calculation, a-SiO_2/Si interface, P_b-type defects, equilibrium density

PACS: 71.15.Mb, 71.20.–b, 61.72.Bb, 61.80.Az **DOI:** 10.1088/1674-1056/ac0e20

1. Introduction

With the development of metal-oxide-semiconductor (MOS) technology, a-SiO_2/Si interface has been widely studied as an important part of semiconductor devices. The threefold-coordinated silicon at a-SiO_2/Si interface is usually called P_b-type defect, that is, there is a Si dangling bond on the side near the Si atom. The hanging bond defects at the interface will affect the performance of the device, which should be minimized in the process of semiconductor device preparation. Hydrogen is usually used to passivate P_b-type defects and inactivate them by forming the saturated dangling bond (P_bH).[1] All P_b-type defects have the similar structure [$\cdot Si(-Si)_3$] and chemical properties. There are three types of P_b defects: P_b, P_{b0}, and P_{b1}. The first one exists in a-SiO_2/Si(111) interface, and the latter two are located at a-SiO_2/Si(100) interface.[2–6]

In the field of defect physics, the microscopic recognition of charge traps at SiO_2/Si(111) interface is implemented by electron paramagnetic resonance (EPR).[3,7–9] Previous works studied the passivation and dissociation kinetics of P_b defects at SiO_2/Si(111) interface by EPR. The kinetic parameters of the thermal passivation in molecular H_2 and dissociation in vacuum of P_b defects were measured.[10–13] No matter passivation or dissociation, it is found that the reaction processes of P_b-type defects are very similar.[14,15] The overall analysis of P_b–hydrogen interaction in SiO_2/Si(111) interface is also applicable to the defects in SiO_2/Si(100) interface.[16] Therefore, Stathis and Stesmans *et al*. measured the kinetic parameters of P_{b0} and P_{b1} defects in the dissociation and passivation reaction processes by EPR.[15,17–19] However, due to the overlapping of the P_{b0} and P_{b1} signals, the activation energy and the pre-exponential factor of the two kinds of defects may not be accurately determined.

For the process of passivation and dissociation of P_b-type defects, the accuracy of the kinetic parameters is affected by some inevitable factors such as spectral interference. In this work, in order to accurately determine the activation energy and pre-exponential factor, the mechanism of passivation and dissociation of P_b-type defects is studied by using the Vienna *ab-initio* simulation package (VASP) code based on the density functional theory (DFT). The reaction rates are calculated by the climbing image nudged elastic band (CI-NEB) method and harmonic transition state theory (HTST). Then, the equilibrium density ratios of the saturated to the unsaturated ones as functions of temperature are calculated by using the reaction kinetic theory coupling the passivation and the dissociation reactions.

*Project supported by the Science Challenge Project, China (Grant No. TZ2016003-1-105), the Tianjin Natural Science Foundation, China (Grant No. 20JCZDJC00750), and the Fundamental Research Funds for the Central Universities, Nankai University (Grant Nos. 63211107 and 63201182).

†Corresponding author. E-mail: xzuo@nankai.edu.cn

© 2021 Chinese Physical Society and IOP Publishing Ltd

2. Computational methods

The a-SiO_2/Si(100) interface and a-SiO_2/Si(111) interface models in this work are derived from previous works.[20–22] They are prepared by molecular dynamics simulation and implemented by the LAMMPS (large scale atomic/molecular massively parallel simulator) code including the ReaxFF force field.

In order to find the reaction curve and activation energy in the passivation and dissociation processes of P_b-type defects, the climbing image-nudged elastic band (CI-NEB) method[23] is hired to search the minimum-energy path (MEP) and exact saddle point, and transition state structure. Firstly, stable initial and final structures are prepared, and then appropriate number of images are inserted between the initial and final structures. The Perdew–Burke–Ernzerhof (PBE)[24] parameterization of the generalized gradient approximation (GGA) exchange correlation is hired in the calculation. The interaction between valence electrons and atomic core are described in terms of the projection augmented plane wave method. The cutoff energy is set to be 520 eV for the plane-wave basis. The precision of electron iteration is 10^{-5} eV, and the precision of ionic loop is controlled by the criterion that the residue force on each atom is less than 0.05 eV/Å.

After the transition state is found, the inactive atoms in the initial state and the transition state are fixed, and the harmonic vibration frequency is calculated. Then, the reaction rate is calculated in terms of the harmonic transition state theory (HTST).[25]

3. Kinetics of passivation and dissociation

Brower quantified the interaction kinetics of P_b and H_2 at SiO_2/Si(111) interface in his early work. The essence of the interaction is the dissociation of H_2 molecule, and P_b acts as a catalyst for the decomposition of H_2 molecule. It is discovered that when temperature is higher than approximately 220 °C, P_b centers are passivated to P_bH in H_2. In addition, when temperature exceeds 550 °C, the passivated centers dissociate in vacuum.[10,14] The passivation and dissociation are described by the equations

$$P_b + H_2 \xrightarrow{k_f} P_bH + H, \tag{1}$$

$$P_bH \xrightarrow{k_d} P_b + H, \tag{2}$$

where k_f is the rate constant of the passivation and k_d is the rate constant of the dissociation. Because H atoms enter vacuum through SiO_2, they have a very high diffusion rate and leave from the interface almost instantaneously. As a result, reverse reactions can be ignored.[16] The reaction rate equations of the passivation and dissociation are as follows:

$$\frac{d[P_b]}{dt} = -k_f[P_b][H_2], \tag{3}$$

$$\frac{d[P_b]}{dt} = k_d(N_0 - [P_b]) = k_d[P_bH], \tag{4}$$

where N_0 is the total density of P_b sites (the maximum number of recoverable ESR active defects),[26] $N_0 \sim 5\times10^{12}$ cm^{-2}, and $[H_2]$ is the volume concentration of H_2 molecules at SiO_2/Si interface. By combining Eqs. (3) and (4), the equilibrium density ratio of $[P_bH]$ to $[P_b]$ is obtained by

$$\frac{[P_bH]}{[P_b]} = \frac{k_f[H_2]}{k_d}, \tag{5}$$

where $[H_2]$ corresponds to the physical solubility of H_2 in vitreous silica, so for the purpose of calculation, it can be approximated by the stretched exponential[16,27]

$$[H_2]\left(\text{cm}^{-3}\cdot\text{atm}^{-1}\right) = 2.639\times10^{17} + 5.439\times10^{21} \times \exp\left\{-\left[\frac{T}{2.415}\right]^{0.4299}\right\}. \tag{6}$$

Therefore, in order to obtain the equilibrium density ratios of $[P_bH]$ to $[P_b]$ as functions of temperature and hydrogen concentration, we only need to know the passivation reaction rate constant k_f and the dissociation reaction rate constant k_d. The passivation and dissociation rate constants are given by the Arrhenius equations[11]

$$k_f = k_{f0}\exp\left(-\frac{E_f}{k_BT}\right), \tag{7}$$

$$k_d = k_{d0}\exp\left(-\frac{E_d}{k_BT}\right), \tag{8}$$

where T is the temperature (in units of K), E_f is the activation energy of the passivation reaction, E_d is the activation energy of the dissociation reaction, k_B is the Boltzmann's constant, and k_{f0} and k_{d0} are the respective pre-exponential factors for passivation and dissociation.

According to the harmonic transition state theory (HTST), the pre-exponential factor is given by

$$k_{HTST} = \frac{\prod_i^{3N}\nu_i^R}{\prod_i^{3N-1}\nu_i^S}\exp\left[-\frac{E^S - E^R}{k_BT}\right], \tag{9}$$

where N is the number of atoms, ν_i^R and ν_i^S are the vibrational frequencies of the ith normal mode at the initial state and transition state, respectively, E^R and E^S are the energies of the initial state and transition state, respectively. The pre-exponential factor is equal to the ratio of the product of the initial state vibration frequencies to the product of the transition state vibration frequencies.[25]

P_{b0} and P_{b1} defects are located at SiO_2/Si(100) interface. Like P_b defect, their passivation and dissociation reactions mainly take place under hydrogen annealing, where the above analysis holds.[14–16] The initial density[28] of P_{b0} and P_{b1} defects is about 1×10^{12} cm^{-2}, and the initial density of P_b defects is about 5×10^{12} cm^{-2}.

4. Results and discussion

4.1. Kinetic parameters of P_b-type defects

4.1.1. Passivation of P_b defects with molecular H_2

The P_b defect is located at SiO_2/Si(111) interface and has a certain effect on the surface states of the semiconductor-oxide interface.[2,29] In the process of annealing,[30] the interface defects will be passivated in H_2. First of all, we calculate the reaction barrier and look for the transition state of the passivation reaction by using the CI-NEB method. The structures of the initial and final states of the passivation reaction are shown in Fig. 1(a). In order to obtain the initial state of the passivation reaction, a hydrogen molecule is placed in the position near the trivalent interfacial silicon atom, and then the atomistic model is relaxed. In order to obtain the final state of the passivation reaction, one hydrogen atom is fixed in the interstitial position near the passivated P_b defect, and the other hydrogen atom is used to passivate the silicon dangling bond.

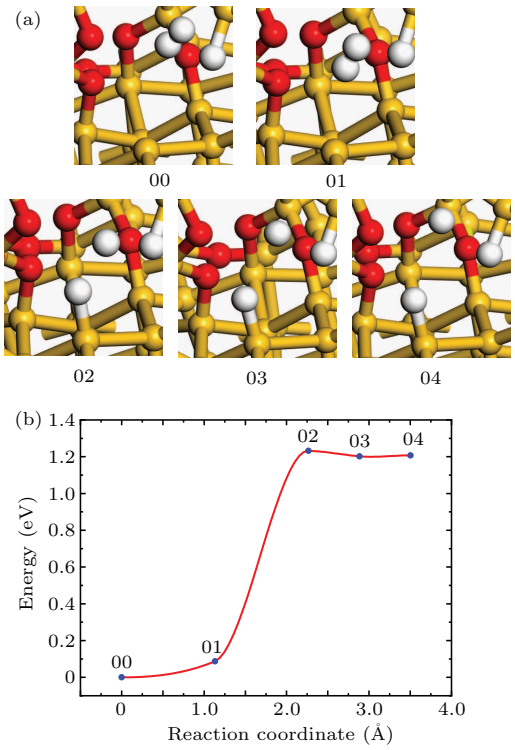


Fig. 1. (a) The atomic structures of the initial (00), final (04), and intermediate (01, 02, and 03) states of the P_b passivation reaction. (b) Reaction curve of the P_b passivation reaction between H_2 and P_b defect.

At the beginning of the reaction, the bond length of the H–H bond in hydrogen molecule is about 0.75 Å. With the reaction proceeding, the distance between the two H atoms increases, and the total energy of the system also increases. When the reaction proceeds to the 02 state, the distance between the two hydrogen atoms is about 1.76 Å, and the distance between the passivating hydrogen atom and the defective silicon atom (Si_d) is 1.52 Å. At this time, the energy reaches the maximum, and the energy increases by 1.23 eV compared with the initial state. With the reaction going on, when the final state is reached, the H and Si_d develop a bond with a bond length of 1.5 Å, which is consistent with the ideal Si–H bond length ($\sim$ 1.5 Å). From the transition state 02 to the final state 04, the total energy of the system decreases by 0.025 eV.

In Fig. 1(b), the 02 state is the transition state and the activation energy is 1.23 eV. The vibrational frequency calculated by VASP software shows that there is no imaginary frequency in the initial state and one and only one imaginary frequency in the transition state. The pre-exponential factor is calculated to be 1.54×10^{-9} $cm^3 \cdot s^{-1}$.

4.1.2. Dissociation of P_bH in vaccum

In the process of annealing in hydrogen-containing ambient, both passivation and dissociation of P_b defects occur.[16] The CI-NEB method is hired to calculate the reaction barrier of the dissociation reaction and to look for the transition state. The structures of the initial and final states of the dissociation reaction are shown in Fig. 2(a). In order to obtain the initial state of the dissociation reaction, a hydrogen atom is moved to the unsaturated dangling bond to passivate the P_b defect, and then the whole model is relaxed. In order to obtain the final state of the dissociation reaction, the hydrogen atom is placed in the void of the a-SiO_2 random network far enough away from the P_b defect, and then the whole model is relaxed.

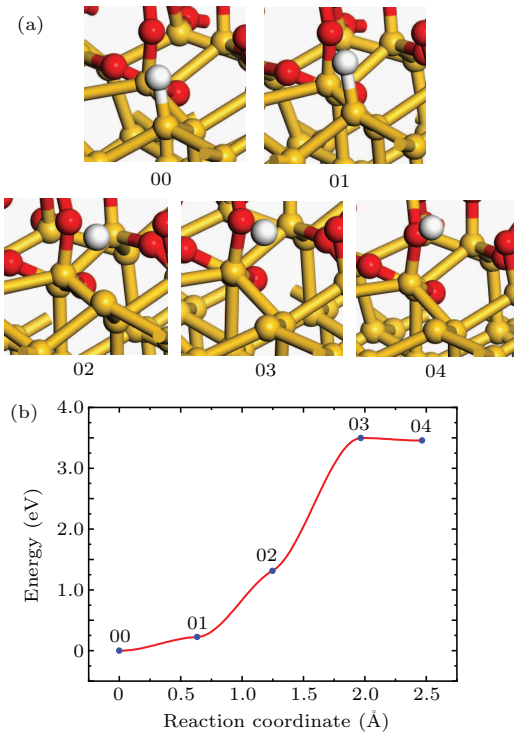


Fig. 2. (a) The atomic structures of the initial (00), final (04), and intermediate (01, 02, and 03) states of the P_b dissociation reaction. (b) Reaction curve of the P_b dissociation reaction between H atom and P_b defect.

At the beginning of the dissociation reaction, the Si–H bond length is 1.5 Å. With the reaction proceeding, the hydrogen atom leaves from the Si_d. With the reaction going on, the distance between the hydrogen atom and the Si_d becomes longer and the energy of the system increases. When the distance between the hydrogen atom and the Si_d is about

2.95 Å, the total energy of the system reaches the maximum about 3.5 eV (transition state 03 in Fig. 2(b)) higher than the initial state. As the reaction proceeds to the final state, the distance between the hydrogen atom and the Si_d is about 3.35 Å, and the total energy of the system decreases by 0.04 eV.

In Fig. 2(b), the 03 state is the transition state and the activation energy is 3.50 eV. The frequency analysis of simple harmonic vibration shows that there is no imaginary frequency in the initial state, and there is one and only one imaginary frequency in the transition state. The pre-exponential factor is 4.12×10^{14} s^{-1}.

Both passivation and dissociation simulated here are strongly endothermic, because a neutral hydrogen atom is produced in the interstitial of the a-SiO_2 random network.

4.1.3. Passivation of P_{b1} defects with molecular H_2

For P_{b1} defects, Stirling *et al.* pointed out that the asymmetrically oxidized dimer (AOD) model is more reasonable than the dimer and bridge model.[31] In the AOD model, two backward Si–Si bonds in the dimer structure are oxidized, which makes the direction of the dangling bond closer to the experimental value. Therefore, the passivation of the AOD model is investigated in this work. The structures of the initial and final states of the P_{b1} passivation reaction are shown in Fig. 3(a). In the passivation process, the passivating hydrogen atom is detached from the hydrogen molecule and approaching to the P_{b1} defect. Due to the interaction between the passivating hydrogen atom and the dangling band Si, the distance between the two hydrogen atoms is increasing, and the total energy of the system increases. When the distance between the two hydrogen atoms is about 1.41 Å and the distance between passivating hydrogen atom and Si_d is about 1.63 Å, the energy increases by 1.19 eV, and the total energy of the system reaches the maximum value (transition state 02 in Fig. 3(b)). As the reaction continues, the distance between passivating hydrogen atom and Si_d becomes shorter, and the total energy of the system decreases by 0.077 eV.

In Fig. 3(b), the state 02 is the transition state and the activation energy is 1.19 eV. The frequency analysis of simple harmonic vibration indicates that there is no imaginary frequency in the initial state and one and only one imaginary frequency in the transition state. The pre-exponential factor is 1.49×10^{-9} $cm^3 \cdot s^{-1}$.

4.1.4. Dissociation of $P_{b1}H$ in vacuum

The structures of the initial and final states of the P_{b1} dissociation reaction are shown in Fig. 4(a). In the process of dissociation reaction, the hydrogen atom will be detached from the passivated Si atom, and the distance between the hydrogen atom and the Si_d becomes longer. In addition, the total energy of the system increases slightly. When the distance between the hydrogen atom and the Si_d is 2.99 Å, the Si_d–H bond is broken, and the total energy of the system reaches the maximum value, which is about 3.58 eV (transition state 03 in Fig. 4(b)). With the reaction going on, the total energy of the system decreases by 0.026 eV, and the distance between hydrogen atom and Si_d reaches about 3.39 Å.

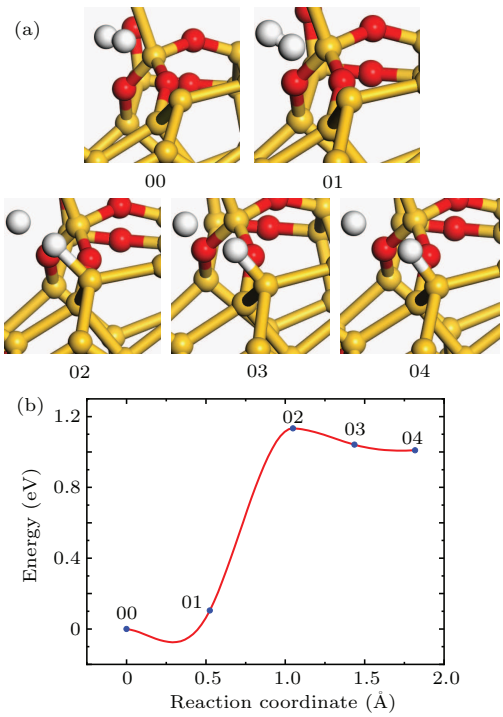


Fig. 3. (a) The atomic structures of the initial (00), final (04), and intermediate states (01, 02, and 03) of the P_{b1} passivation reaction. (b) Reaction curve of the P_{b1} passivation reaction between H_2 and P_{b1} defect.

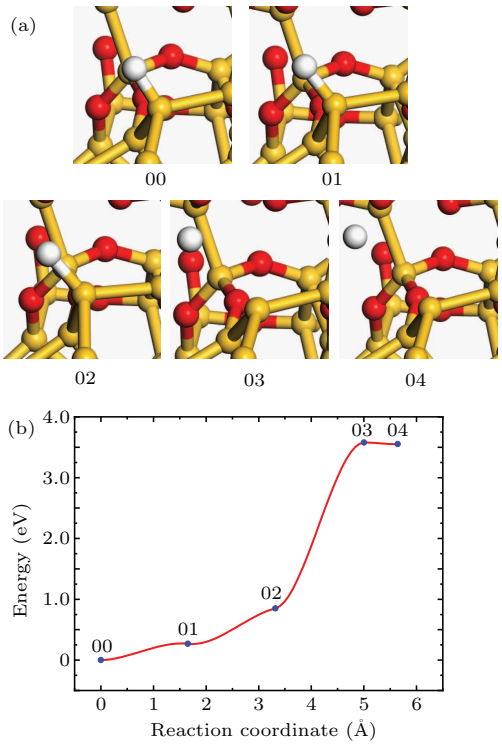


Fig. 4. (a) The atomic structures of the initial (00), final (04), and intermediate (01, 02, and 03) states of the P_{b1} dissociation reaction. (b) Reaction curve of the P_{b1} dissociation reaction between H atom and P_{b1} defect.

In Fig. 4(b), the 03 state is the transition state and the activation energy is 3.58 eV. The results of frequency calculation demonstrate that there is no imaginary frequency in the initial state and one and only one imaginary frequency in the transition state. The pre-exponential factor is 2.33×10^{14} s^{-1}.

4.1.5. Passivation of P_{b0} defects with molecular H_2

In addition to P_{b1} defects, there are P_{b0} defects in a-SiO_2/Si(100) interface. The P_{b0} defect is located in the second layer of silicon atom beneath the interface.[32] The structures of the initial and final states of the P_{b0} passivation reaction are shown in Fig. 5(a). In the passivation process, the passivating hydrogen atom is detached from the hydrogen molecule and approaching to the P_{b0} defect. Due to the Coulomb interaction between the hydrogen atom and the Si_d, the distance between the hydrogen atom and Si_d is getting closer, the distance between two hydrogen atoms is increasing, and the total energy of the system is rising. Subsequently, the H–H bond is broken and the hydrogen atom near the defect is covalently bonded to the Si_d (transition state 02 in Fig. 5(b)). Meanwhile, the distance between the two hydrogen atoms is about 1.40 Å, and the distance between the passivating hydrogen atom and the Si_d is 1.72 Å. With respective to the initial state, the total energy of the system increases by 1.13 eV. With the reaction going on, the distance between the hydrogen atom and the Si_d gradually becomes shorter, and the total energy of the system decreases by 0.123 eV.

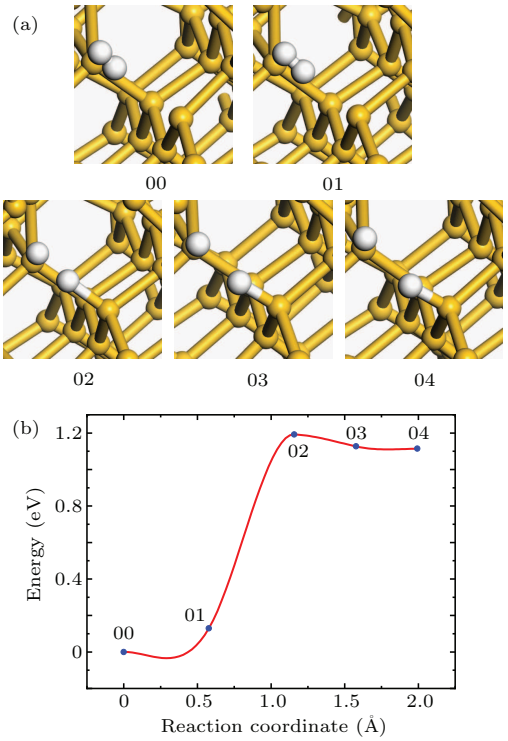


Fig. 5. (a) The atomic structures of the initial (00), final (04), and intermediate (01, 02, and 03) states of the P_{b0} passivation reaction. (b) Reaction curve of the P_{b0} passivation reaction between H_2 and P_{b0} defect.

In Fig. 5(b), the state 02 is the transition state and the activation energy is 1.13 eV. The results of frequency analysis display that there is no imaginary frequency in the initial state and one and only one imaginary frequency in the transition state. The pre-exponential factor is 2.49×10^{-8} $cm^3 \cdot s^{-1}$.

4.1.6. Dissociation of $P_{b0}H$ in vaccum

Compared to P_{b1} defect, the dissociation of P_{b0} defect is more complicated. Because the atomic structure around a P_{b0} defect is similar to that of crystalline silicon, the dissociated hydrogen atom is easily trapped by a Si–Si bond during the dissociation process, forming the stable hydrogen bridge structure (Si–H–Si). The structures of the initial and final states of the dissociation reaction are shown in Fig. 6(a). A hydrogen atom is transferred to the unsaturated dangling bond to passivate the P_{b0} defect. After structural relaxation, the initial state structure of the P_{b0} defect dissociation reaction is obtained. The hydrogen atom is placed next to the Si–Si bond near the defect, and the final state structure of P_{b0} defect dissociation reaction is obtained by structural relaxation.

In the process of dissociation, the hydrogen atom is separated from the Si_d. As the reaction continues, the distance between the hydrogen atom and the Si_d becomes longer and the total energy of the system increases. In the 03 state, the covalent bond between the hydrogen atom and the Si_d is broken. In addition, the hydrogen atom is bonded with Si(1), and the length of Si(1)–H bond is about 1.76 Å. In the 04 state, the distance between the hydrogen atom and the Si_d is about 2.67 Å, and the Si(1)–H bond length is about 1.58 Å. The energy of the system reaches the maximum value, which increases by about 2.25 eV. In the 05 and 06 states, the atomic structures around Si(1) and Si(2) continue to relax. When the distance between the hydrogen atom and the Si_d reaches about 3.75 Å, the hydrogen atom is bonded with both Si(1) and Si(2) forming the hydrogen bridge structure, and the total energy of the system decreases by 0.295 eV. The Si(1)–H bond length is about 1.61 Å, and the Si(2)–H bond length is about 1.65 Å.

In Fig. 6(b), the 04 state is the transition state and the activation energy is 2.25 eV. The results of the frequency analysis show that there is no imaginary frequency in the initial state and one and only one imaginary frequency in the transition state. The pre-exponential factor is 5.99×10^{13} s^{-1}.

Compared to P_b and P_{b1} defects, the forward reaction barrier of P_{b0} defect is obviously lower. Through Bader charge analysis of the dissociation process of P_b, P_{b0}, and P_{b1} defects, it is found that the initial states of the dissociation reactions for the three defects are basically similar: the valence electron numbers of the three passivated Si atoms are 3.34, 3.39, and 3.15, respectively. The valence electron number of the passivating hydrogen atoms of the three defects are 1.55, 1.59, and 1.55, respectively. For the three defects, the final states of the dissociation reactions are slightly different: the valence electron numbers of the three defects are 3.98, 3.87, and 3.91, respectively. The valence electron numbers of the passivating hydrogen atoms of the three defects are 0.99, 1.64, and 0.99,

respectively. Therefore, the charge transfer of P_{b0} dissociation is very different from that of P_b and P_{b1}. The final state of the P_{b0} dissociation produces the more stable hydrogen bridge structure, which makes the hydrogen atom negatively charged. This may be the reason why the forward reaction barrier of the P_{b0} dissociation reaction is lower.

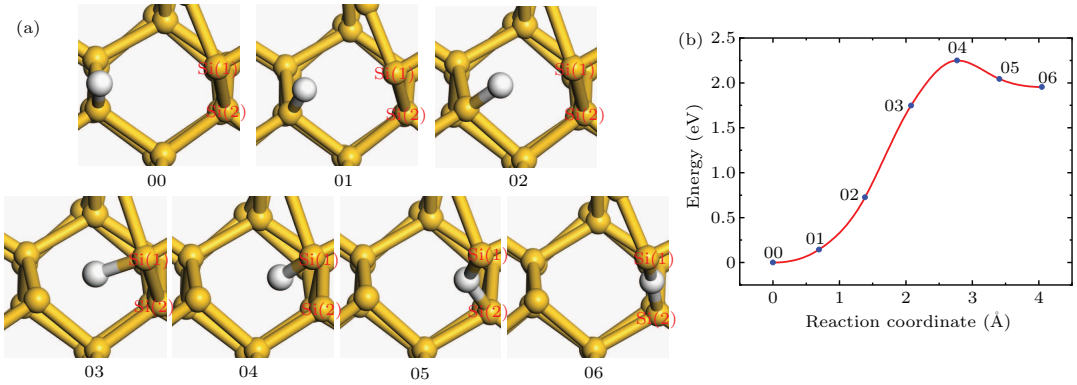


Fig. 6. (a) The atomic structures of the initial (00), final (06), and intermediate (01, 02, 03, 04, and 05) states of the P_{b0} dissociation reaction. (b) Reaction curve of the P_{b0} dissociation reaction between H atom and P_{b0} defect.

4.2. Equilibrium density ratio of saturated interface dangling bond and intebrface defect

The calculated values of this work are compared with the experimental values in Tables 1 and 2. The calculated results of this work agree well with the experimental values. σ_{E_f} and σ_{E_d} are spreads in activation energies around the mean values E_f and E_d for passivation and dissociation, respectively. The spreads are found adequately described by Gaussian distributions in the generalized simple thermal (GST) model.[16] In the passivation reactions of the three kinds of defects, the activation energies are approximately equal and $P_b > P_{b1} > P_{b0}$. In the dissociation reactions, the activation energies of P_b and P_{b1} are approximately equal, but the activation energy of the P_{b0} defect is lower than them by about 1 eV. Because the hydrogen atom generated by the P_{b0} dissociation reaction is not standing alone in bulk silicon and forms the stable hydrogen bridge (Si–H–Si) structure, the activation energy of the dissociation reaction is reduced. In addition, the pre-exponential factors k_{f0} of the passivation reactions of the three kinds of defects are relatively close to each other and $P_{b0} > P_b > P_{b1}$, in which the pre-exponential factor of P_{b0} passivation reaction is one order of magnitude larger than that of P_b and P_{b1}. The pre-exponential factors k_{d0} of dissociation reactions are also close to each other and $P_b > P_{b1} > P_{b0}$, where the pre-exponential factor of P_{b0} dissociation reaction is one order of magnitude smaller than that of P_b and P_{b1}. This result may be determined by the structure of the defect itself. It is worth noting that the pre-exponential factors of the passivation reactions of P_{b0} and P_{b1} calculated in this work are slightly lower than the experimental values, possibly because of the fact that the signals of P_{b0} and P_{b1} defects overlap each other, resulting in spectral interference.[19]

We set the temperature range of 600–1000 °C with an interval of 20 °C, and substitute it into Eq. (6) to obtain the solubility of H_2 in SiO_2 at different temperatures. The calculated activation energies and pre-exponential factors of the passivation and dissociation reactions of the P_b-type defects are substituted into Eqs. (7) and (8) to obtain the reaction rate constants k_f and k_d at different temperatures. By substituting k_f, k_d, and $[H_2]$ into Eq. (5), the equilibrium density ratio of the saturated interfacial dangling bonds and interface defects under the impact of both passivation and dissociation is obtained, as shown in Fig. 7.

Table 1. Summary of the kinetic parameters for passivation reactions of P_b-type defects.

		E_f (eV)	σ_{E_f} (eV)	k_{f0} (cm^3·s^{-1})
P_b	This work	1.23	0	1.54×10^{-9}
	[a]Exp.	1.51 ± 0.04	0.06 ± 0.004	$9.8(+8/-5)\times10^{-8}$
P_{b0}	This work	1.13	0	2.49×10^{-8}
	[b]Exp.	1.51 ± 0.04	0.14 ± 0.02	$1.43(\pm0.6)\times10^{-6}$
P_{b1}	This work	1.19	0	1.49×10^{-9}
	[b]Exp.	1.57 ± 0.04	0.15 ± 0.03	$1.43(\pm0.6)\times10^{-6}$

[a]Ref. [12], [b]Ref. [19].

Table 2. Summary of the kinetic parameters for dissociation reactions of P_b-type defects.

		E_d (eV)	σ_{E_d} (eV)	k_{d0} (s^{-1})
P_b	This work	3.50	0	4.12×10^{14}
	[c]Exp.	2.83 ± 0.03	0.08 ± 0.03	$1.6(\pm0.5)\times10^{13}$
P_{b0}	This work	2.25	0	5.99×10^{13}
	[d]Exp.	2.86	0	2×10^{13}
P_{b1}	This work	3.58	0	2.33×10^{14}
	[d]Exp.	2.91	0	2×10^{13}

[c]Ref. [13], [d]Ref. [15].

It is shown in Fig. 7 that the equilibrium density ratio of the saturated interfacial dangling bonds to the interfacial defects monotonically decreases with the increase of temperature in the range of 600–1000 °C. It is consistent with Stesman's view that more effective passivation requires longer passivation at lower temperatures.[16] Among the P_b-type defects, the value of $[P_{b1}H]/[P_{b1}]$ is always the largest, the value of $[P_bH]/[P_b]$ is the second, and the value of $[P_{b0}H]/[P_{b0}]$ is the smallest. At 600 °C, the maximum of $[P_{b1}H]/[P_{b1}]$ is about 1.09×10^8, that of $[P_bH]/[P_b]$ is about 1.29×10^7, and that of $[P_{b0}H]/[P_{b0}]$ is about 3.36×10^2. At 1000 °C, the value of

$[P_{b1}H]/[P_{b1}]$ is about 4.78×10^3, that of $[P_bH]/[P_b]$ is about 9.37×10^2, and that of $[P_{b0}H]/[P_{b0}]$ is about 2.96. This is because the activation energy of P_{b0} dissociation reaction is much lower than those of P_b and P_{b1}. In Arrhenius formula, the activation energy is in the exponential position, and a relatively low activation energy will lead to a significant increase in the rate constant of the dissociation reaction. It is obvious in Eq. (5) that the $[P_{b0}H]/[P_{b0}]$ is inversely proportional to the dissociation rate constant k_d. This result is consistent with that of Stathis *et al.*[33,34] Because P_{b0} defect is located in the second atomic layer beneath the transition region, P_{b0} defect is more difficult to be passivated than P_{b1} defect.

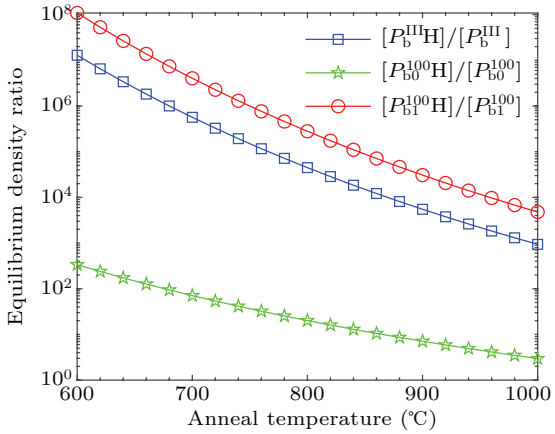


Fig. 7. Equilibrium density ratio of saturated interfacial dangling bonds and interfacial defects of P_b-type defects at 1 atm H_2.

5. Conclusion

Firstly, based on the kinetic theory of P_b–hydrogen reactions, it is deduced that the ratio of equilibrium density of the saturated interfacial dangling bonds to interfacial defects is a function (Eq. (5)) of reaction rate constants k_f and k_d. Secondly, the reaction mechanisms of passivation and dissociation of the P_b-type defects are investigated by using first-principles calculations based on density functional theory. The activation energies and transition states of the passivation and dissociation reactions of P_b-type defects are calculated by the CI-NEB method. According to the harmonic transition state theory (HTST), the harmonic vibration frequency of the initial state and transition state is analyzed, and the pre-exponential factor is calculated. The calculated results are essentially consistent with the previous experimental values. Finally, the calculated activation energy and pre-exponential factor are substituted into the Arrhenius formula to obtain the reaction rate constant, and the reaction rate constant is substituted into Eq. (5) to obtain the equilibrium density ratio of the saturated interfacial dangling bonds and interfacial defects.

In the passivation reactions, the passivating hydrogen atom is detached from the hydrogen molecule and approaching to the interface defect to passivate the dangling bond defect. In the dissociation reactions, the hydrogen atom breaks away from the three-fold coordinated silicon atom and reaches the void near the interface defects. However, the hydrogen atom in the P_{b0} dissociation reaction can be easily trapped by a Si–Si bond, forming the Si–H–Si hydrogen bridge structure. The simulation results show that the passivation and dissociation reactions of P_b-type defects are endothermic, and the forward reaction barrier is much higher than the reverse one.

In brief, the activation energies and pre-exponential factors of the passivation and dissociation reactions of the P_b-type defects are calculated by using first-principles calculations and in good agreement with the experimental values. It is shown that the ratio of equilibrium density of the saturated interfacial dangling bonds to interfacial defects follows the order $P_{b1} > P_b > P_{b0}$. When the temperature is between 600 °C and 1000 °C, the passivation degree of P_b type defects monotonically decreases with the increase of temperature. Among them, the passivation degree of P_{b0} is the lowest.

References

[1] Cheng Y C 1977 *Prog. Surf. Sci.* **8** 181
[2] Caplan P J, Poindexter E H, Deal B E and Razouk R R 1979 *J. Appl. Phys.* **50** 5847
[3] Brower K L 1983 *Appl. Phys. Lett.* **43** 1111
[4] Rabedeau T A, Tidswell I M, Pershan P S, Bevk J and Freer B S 1991 *Appl. Phys. Lett.* **59** 3422
[5] Rong F C, Harvey J F, Poindexter E H and Gerardi G J 1993 *Appl. Phys. Lett.* **63** 920
[6] Von Bardeleben H J, Schoisswohl M and Cantin J L 1996 *Colloids Surf. A* **115** 277
[7] Nishi Y, Tanaka K and Ohwada A 1972 *Jpn. J. Appl. Phys.* **10** 52
[8] Lenahan P M and Dressendorfer P V 1982 *Appl. Phys. Lett.* **41** 542
[9] Cook M and White C T 1987 *Phys. Rev. Lett.* **59** 1741
[10] Brower K L 1988 *Phys. Rev. B* **38** 9657
[11] Brower K L and Myers S M 1990 *Appl. Phys. Lett.* **57** 162
[12] Stesmans A 1996 *Appl. Phys. Lett.* **68** 2723
[13] Stesmans A 2000 *Phys. Rev. B* **61** 8393
[14] Brower K L 1990 *Phys. Rev. B* **42** 3444
[15] Stathis J H 1995 *J. Appl. Phys.* **77** 6205
[16] Stesmans A 2000 *J. Appl. Phys.* **88** 489
[17] Khatri R, Asoka Kumar P, Nielsen B, Roellig L O and Lynn K G 1994 *Appl. Phys. Lett.* **65** 330
[18] Van de Walle C G and Street R A 1994 *Phys. Rev. B* **49** 14766
[19] Stesmans A 1996 *Appl. Phys. Lett.* **68** 2076
[20] Li P, Song Y and Zuo X 2019 *Phys. Status Solidi RRL* **13** 1800547
[21] Li P, Chen Z H, Yao P, Zhang F J, Wang J W, Song Y and Zuo X 2019 *Appl. Surf. Sci.* **483** 231
[22] Hong Z C and Zuo X 2020 *Journal of System Simulation* **32** 2362
[23] Henkelman G, Uberuaga B P and Jonsson H 2000 *J. Chem. Phys.* **113** 9901
[24] Perdew J P, Burke K and Ernzerhof M 1996 *Phys. Rev. Lett.* **77** 3865
[25] Vineyard G H 1957 *J. Phys. Chem. Solids* **3** 121
[26] Stesmans A 1993 *Phys. Rev. B* **48** 2418
[27] Shelby J E 1977 *J. Appl. Phys.* **48** 3387
[28] Stesmans A and Afanas'ev V V 1998 *J. Phys.: Condens. Matter* **10** L19
[29] Cook M and White C T 1988 *Phys. Rev. B* **38** 9674
[30] Pantelides S T, Rashkeev S N, Buczko R, Fleetwood D M and Schrimpf R D 2000 *IEEE Trans. Nucl Sci.* **47** 2262
[31] Stirling A and Pasquarello A 2005 *J. Phys.: Condens. Matter* **17** S2099
[32] Stirling A, Pasquarello A, Charlier J and Car R 2000 *Phys. Rev. Lett.* **85** 2773
[33] Stathis J H and Cartier E 1994 *Phys. Rev. Lett.* **72** 2745
[34] Stathis J H and Dori L 1991 *Appl. Phys. Lett.* **58** 1641